Chapter@4

Influence of amine modified graphene on polyurethane properties

4.1 Introduction:

Polyurethane (PU), a novel polymeric material, is used in biomedical application because of its biocompatibility, easy processibility and better mechanical strength which are close to the properties of natural tissues [Lan et al. (1996); Guan et al. (2005)]. Polyurethanes (PU) are extensively used as adhesives, synthetic leather [Deka et al. (2009)], foam [Saha et al. (2008)], coatings [Park et al. (2002)], construction material, flame retardants [Cyriac et al. (2011)], wound dressing [Xu et al. (2013)], and other biomedical applications [Camposa et al. (2011)]. Along this polyurethane composites show superior tribological and wear resistant properties over the metals and ceramics which make it a suitable material for triobological and marine applications. It can be synthesized by polyaddition reaction of polyol, diisocyanate and chain extender. Properties of the polymer can be altered by changing the composition and nature of ingredient used during the synthesis or by incorporation of filler in polymer matrix [Mishra et al. (2010)]. Polyurethane consists of hard and soft segment units and these segments determine the property of overall polymer. Self–assembly which is a common phenomenon occurred in block copolymer [Jain et al. (2003)] and dendritic polymer [Bosman et al. (1999); Gillies et al. (2004)] is also reported in aliphatic polyurethane which play very important role in altering the properties of the polymer. Self–assembled polymeric materials show the better thermal as well as the mechanical stabilities over the conventional micelles and are expected to enhance the biological activities of the polymer as well [Discher et al. (1999)].

A wide range of the nanoparticles including metal and its oxide [Saint et al. (1998); Gupta et al. (2005)], nanoclay [Wang et al. (1998)], CNTs [Koerner et al.

(2004)] in different forms are being frequently used for modification of structure, mechanical and biological properties of the polymer [Zhang et al. (2010)]. Recently, graphene, sp^2 hybridized carbonious material, has drawn tremendous attention in the field of hybrid materials due to its exceptional thermal [Balandin et al. (2008)], mechanical [Dikin et al. (2007)], optical [Rao et al. (2009)] and electrical properties [Tombros et al. (2007)]. Graphene or its derivatives are frequently used in composites materials [Bai et al. (2010)] , sensor [Lu et al. (2009)], catalysis [Qu et al. (2010)], electronics [Xuan et al. (2008)], and as a carrier for drug or gene in biomedical fields [Liu et al. (2008)]. Due to its high aspect ratio, graphene provides the large interfacial area to the polymer for interaction which helps to improve the pristine properties of the polymer [Xu et al. (2001)]. There are several reports [Wu et al. (2012), Nguyen et al. (2009)]of polyurethane composite materials containing graphene as the filler, but most of them are physical mixture of graphene (sometimes functionalized) and PU. Incorporation of graphene within the polymer chain is a new idea to make nanocomposites where graphene moieties are chemically connected with polyurethane chains.

This chapter reveals the important effect especially on biological activity of polyurethane when graphene is chemically tagged with polymer chain in comparison to the properties when same graphene is physically dispersed in polyurethane matrix. Chemically tagged nanocomposite is assigned as PUG-C whereas physically mixed is describes as PUG-P. Chemical tagging has been conformed through NMR and other spectroscopic techniques. Comparative study of physical blend of graphene and PU

with the chemically tagged modified graphene within polyurethane chains in terms of interaction, morphological feature, structure and thereby biological applications. Interaction between the polymer matrix and amine modified graphene oxide is monitored through FTIR, UV-visible and PL spectroscopy and demonstrate the interaction and differentiate the two types of nanocomposites containing similar extent of nanofiller. Significant improvements in thermal as well as mechanical properties of nanocomposites are reported and considerable improvement occurs in chemically tagged nanocomposites in comparison to conventional nanocomposites. Biodegradation has been studied showing sustained degradation in nanocomposites vis-à-vis pure polymer usually observed. Graphene induced self–assembly has been explored using nanometer to micron size inhomogeneities and their effects on the drug release study and other biological aspects including biocompatibility and cell adhesion have been explored in detail to find the efficacy of the chemical tagging of graphene within the polyurethane chains. Developed nanocompoosites exhibits good biocompatible nature having sustained release of drug find this class of material superior as compared to conventional composites using same filler.

4.2 Results and Discussion:

4.2.1 Functionalized graphene as chain extender:

Amine functionalized graphene has been dispersed in polyurethane matrix in two different ways i) physical dispersion where graphene sheets are distributed in PU matrix like conventional composite through solution, and ii) chemical dispersion where graphene sheets are chemically tagged with polyurethane chains using amine functionalized graphene as chain extender for the synthesis of PU as mentioned in the experimental section (Scheme 2.3). The formation of chemically tagged graphene oxide nanocomposite has been confirmed from NMR spectroscopy arising from the new peak at δ = 8.17ppm at lower field due to >N–H proton adjacent to the graphene sheet (Figure 4.1). ^{1}H signal for regular >N–H group present in urethane linkages appears at δ = 7.0ppm both for pure PU and composites while the peak intensity has reduced considerably for chemically tagged nanocomposites due to its lower abundance as half of the –NCO groups of diisocyanate is chemically linked to amine functionalized graphene. Further, the high field peaks associated with methylene groups (–CH_2–) either in hexamethylene diisocyanate or polyol have split into couple of peaks in chemically tagged graphene nanocomposites (PUG-C) due to change of electronic environment linked with amine functionalized graphene. On contrary, there is no splitting or shifting of peaks occurs in physically tagged nanocomposite (PUG-P) as compared to pure PU.

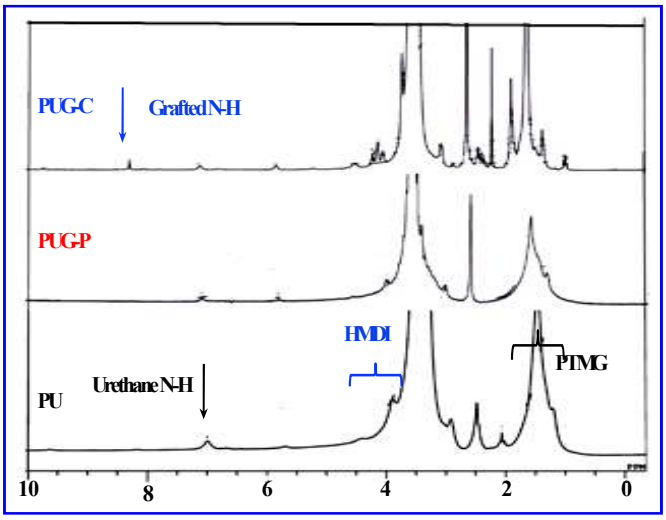

Figure 4.1: ^{1}H-NMR spectra of the pure PU and its indicated nanocomposites.

4.2.2 Nanostructure and interactions:

Physically mixed nanocomposites (PUG-P) are prepared by the addition of modified graphene at the end of the polymerization process followed by mixing for long time which shows highly agglomerated nanostructure of graphene sheet (Figure 4.2a). On the other hand, chemically grafted graphene nanocomposites (PUG-C), synthesized using amine functionalized graphene as chain extender, exhibit homogeneous dispersion of graphene sheets in PU matrix and is expected to show better properties as compared to PUG-P for similar content of graphene. Chemical tagging of graphene within the polyurethane chain has significant influence on the nature of interactions. FTIR and UV-visible spectra of modified graphene oxide are (Figure 4.2b and c). Appearance of the FTIR band at 1571 cm^{-1} in modified graphene indicates the presence of >N–H moiety in amine functionalized graphene after the treatment with ammonia with the disappearance of C–OH and >C=O peaks of graphene oxide at 1398 and 1745

cm^{-1}, respectively [Lai et al. (2011)]. The addition of ammonia solution to graphene oxide suspension also promote the dehydration reaction by removing the hydroxyl groups. Due to this reorganization in the structure of modified graphene (GM), it goes back towards the pristine graphene as verified from the shifting of UV-visible peak to 273 nm from the peak at 307 nm of graphene oxide.

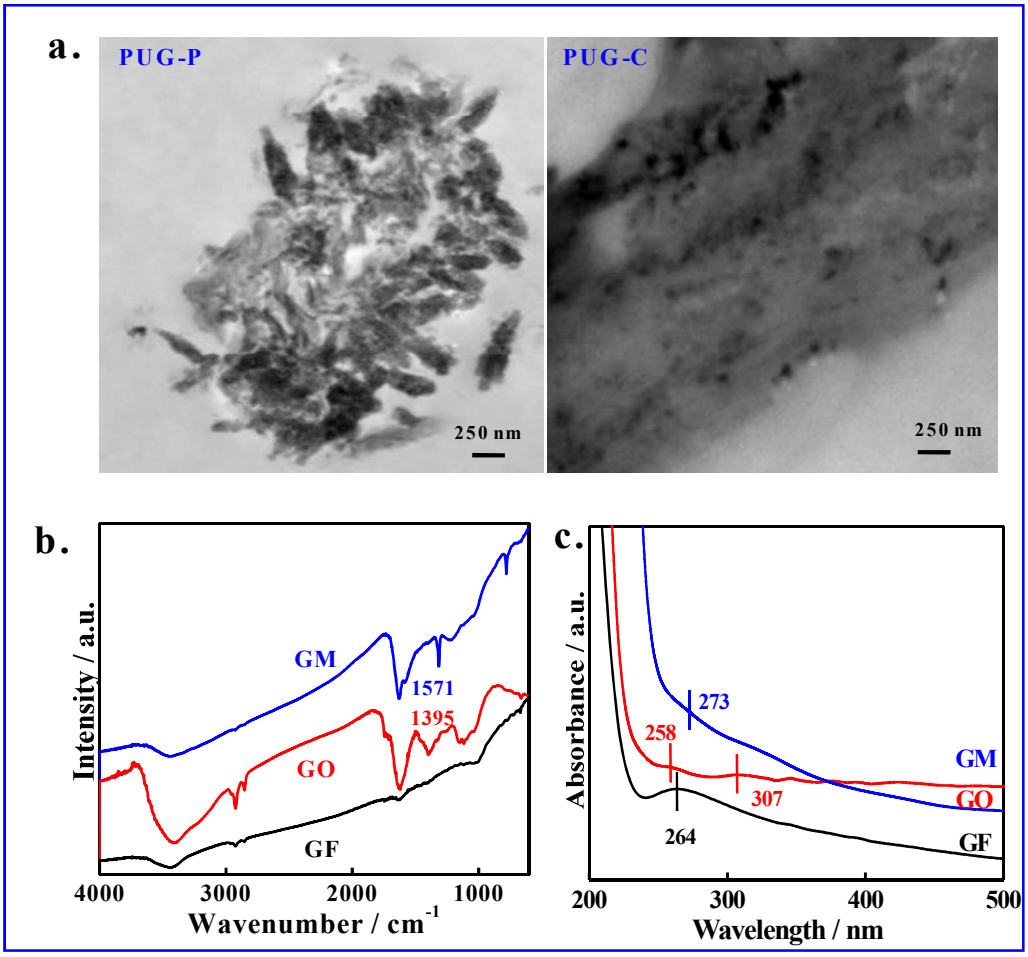

Figure 4.2: (a) Bright filed transmission electron microscope image of indicated; nanocomposites; **(b)** FTIR spectra of amine modified graphene oxide with graphene oxide and graphite flake and **(c)** UV-visible spectra amine modified graphene oxide, graphene oxide and graphite.

Pure polyurethane shows an FTIR absorption peak at 1680 cm^{-1} due to hydrogen bonded urethane moiety which remains unchanged in physically tagged graphene nanocomposite while there is slight shift observed in free >N–H stretching frequency in PUG-P (Figure 4.3). [Patel et al. (2015)]. On the other hand, hydrogen bonded peak has significantly been reduced in chemically tagged nanocomposites (PUG-C) with considerable shift occurs for free >N–H stretching frequency in presence of adjacent constrained graphene moiety**.** Slight shift in hydrogen bonded peak reflects greater interaction between hard segment >N–H group of PUG-C and rest of the polymer chain. The shifting of >N–H stretching frequency for PUG-C to 3325 cm^{-1} from the original peak position at 3319 cm^{-1} for pure PU also suggest strong interaction between graphene sheet and polymer chain against unaltered frequency for PUG-P.

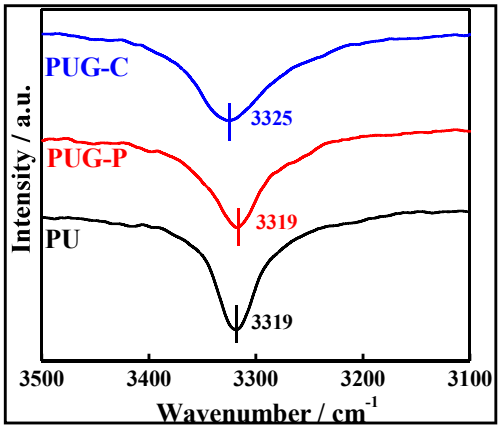

Figure 4.3: FTIR spectra of pure PU and its indicated nanocomposites in –N-H frequency range.

Two nanocomposites are developed, i) by dispersing the graphene sheet in polymer through solution route where the nanofillers are physically adhered with polymer matrix, and ii) graphene sheets become part of long polymer chain by using amine

functionalized graphene as chain extender where individual graphene sheets are homogeneously distributed in PU matrix against the agglomerated nanostructure noticed in physically dispersed nanocomposites (PUG-P). Because of good dispersion and being part of polymer chain, graphene sheets are in good interaction with polymer predominantly through dipolar interaction between π-electron cloud of graphene sheet and the urethane linkages of PU which is reflected in spectroscopic measurements. Extensive hydrogen bonding occurs in pure PU amongst the urethane linkages provide a strong FTIR peak at 1680 cm^{-1} and maintain the intensity of free >N–H group minimal while the free >N–H absorption is prominent at 1725 cm^{-1} with considerable shifting in PUG-C as amine groups in proximity to graphene sheets are unable to form hydrogen bond (Figure 4.4a). Further, better interactions in chemically linked graphene with polyurethane chain is evident from the greater red shift either in UV-vis absorption or emission spectroscopy as compared to physically adhered graphene to PU chains.Further, prominent red shift occurs for nanocomposites due to $\pi \rightarrow \pi^*$ transition in UV-vis absorption spectra as compared to pure PU also confirm good interaction between graphene and polymer chains (Figure 4.4b) [Bhattacharya et al. (2014)]. Moreover, larger shifting in PUG-C verify greater interaction when graphene is chemically tagged with the PU chain vis-à-vis physical dispersion of graphene in PUG-P. (Figure 4.4c) represents the photoluminescence spectra of polyurethane and its nanocomposites excited at 275 nm, as decided from the absorption spectra. Both the nanocomposites show broad PL emission spectra originated from $\pi^* \rightarrow \pi$ transition of graphene moiety [Kumar et al. (2014)]. This peak position of the transition is shifted

towards higher wavelength (393 to 402 nm from graphene to PUG-C) due to electronic redistribution arising from greater interactions between polymer chain and modified graphene against no change of peak position observed in PUG-P. Appearance of the peak band at 441 nm in GM and nanocomposites is due to n→π transition and no shifting is observed in the emission pattern. This is worthy to mention that emission pattern from PU is reflected in the nanocomposites as wider spectrum as compared to modified graphene spectra. Generation of the lower wavelength peak band at 319 nm is reported as the coupling between the $\pi^{*}\rightarrow \pi$ and $n\rightarrow \pi$ transition [Kumar et al. (2014)].

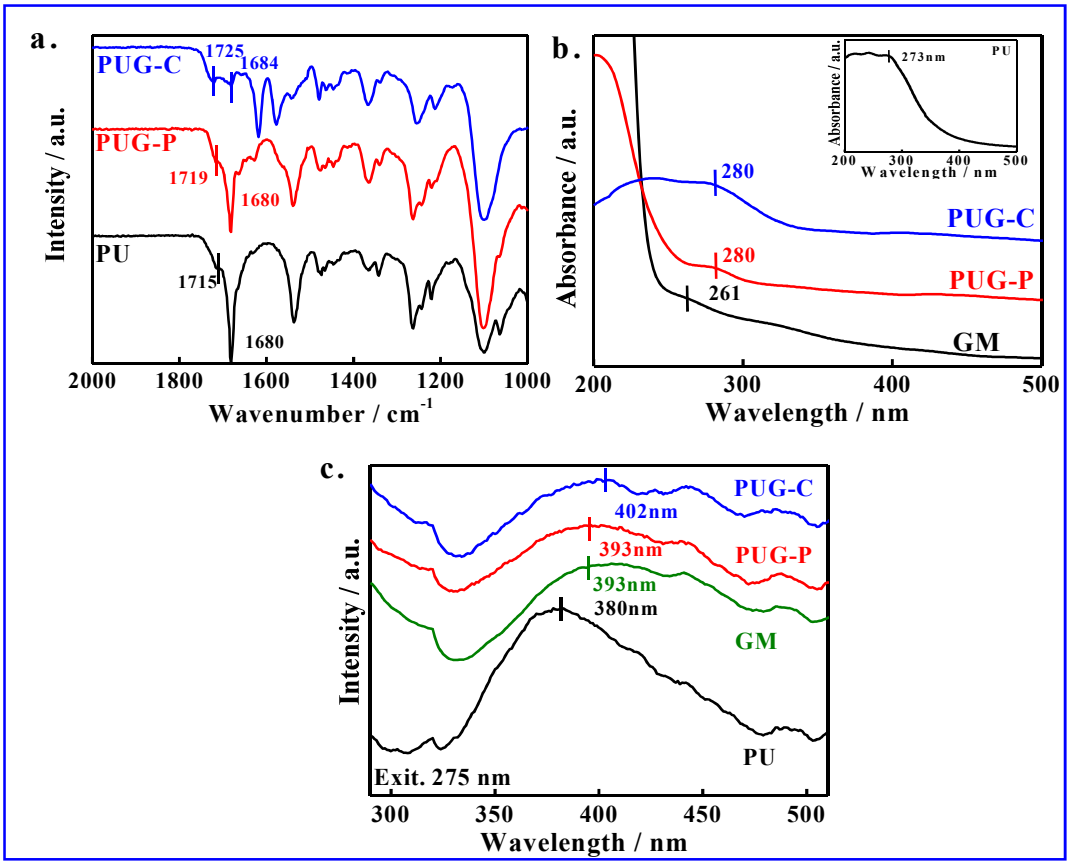

Figure 4.4: (a) FTIR Spectra of the pure PU and its indicated nanocomposites. **(b)** UV-visible spectra of the modified graphene with physically and chemically tagged nanocomposites. (uv-visible spectra of pure PU Inset) and **(c)** PL spectra of pure PU and its indicated nanocomposites with modified graphene.

4.2.3 Effect of graphene on structure, stability and morphology:

(Figure 4.5a) shows the XRD patterns of pure PU and its nanocomposites indicating crystalline structure of pure PU while the crystallinity significantly reduces in nanocomposites. Pure PU exhibits a sharp peak at 24.8^{o} presumably due to crystallinity arises from hard segment zone whose intensity decreases in nanocomposites indicating the amorphous nature even in hard segment region mainly because of the constraints from graphene sheet which do not allow the polymer chain to get crystallized . Further, the peak at 22.3^{o} becomes broader in nanocomposites as compared to pure PU and this broadening is more pronounced in chemically grafted nanocomposites suggesting even more reduction of crystallinity. DSC thermograms of pure PU and its nanocomposites show double endothermic peaks for soft and hard segment melting (Figure 4.5b). Lower endothermic peaks represent the melting behavior of soft segment arising from diol while higher endothermic peaks are responsible for the melting of hard segment [Rogulska et al. (2007)]. Heat of fusion corresponding to hard segment zone remains similar (~6 J.g^{-1}) for pure PU and PUG-P while considerable reduction occurs in PUG-C as graphene sheet adjacent to hard segment do not allow the polymer chains to crystallize in case of chemically tagged nanocomposite. On the other hand, heat of fusion values for soft segment melting increase as 18, 26 and 28 J.g^{-1} for PU, PUG-P and PUG-C, respectively, indicating the nucleating behavior of graphene towards the crystallization of soft segment.

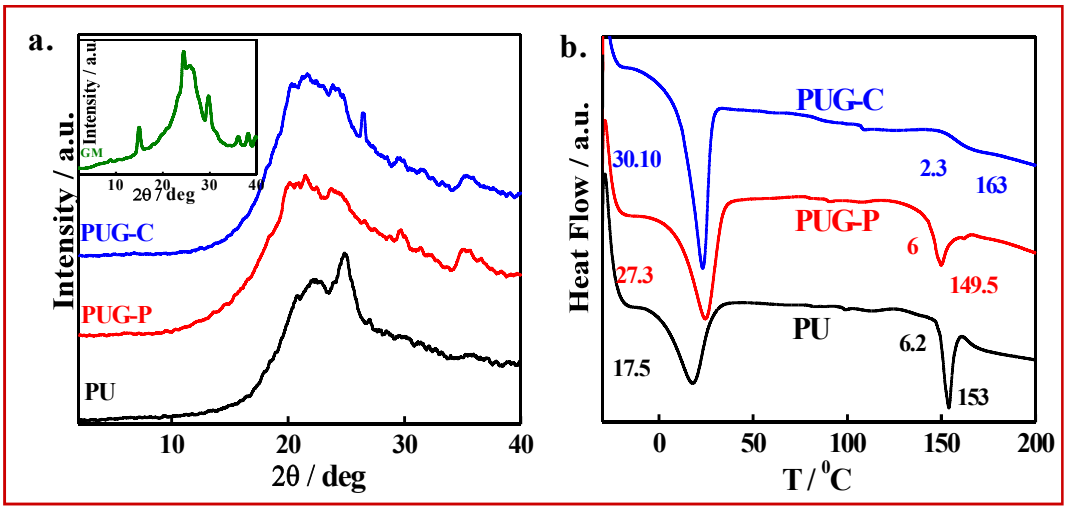

Figure 4.5: (a) XRD pattern of the pure PU and its indicated nanocomposites. (XRD of modified graphene inset) **(b)** DSC thermograph of pure polyurethane and its nanocomposites.

(Figure 4.6a) represents the thermal stability of PU and its nanoomposites against temperature measured using thermogravimetric analyzer. The degradation temperatures, corresponding to the weight loss of 5%, occur at 285, 310 and 343 ºC for PU, PUG-P and PUG-C, respectively, indicating much greater stability of polymer chains in presence of graphene sheets. Higher thermal stability (by more than 50 ºC) of chemically tagged nanocomposites is due to homogeneous dispersion of thermally stable graphene layers in polymer matrix. Moreover, two stages of degradation are observed both for pure polymer and its nanocomposites due to the degradation of hard and soft segment separately and the hard segments being susceptible towards temperature degrades at lower temperature followed by degradation of soft segment at higher temperature [Rogulska et al. (2007)]. Interestingly, the slope of degradation kinetics of PUG-C hard segment is considerably lower against the steep degradation noticed in pure PU due to significantly less aggregation of hard segment as discussed

above in case of chemically tagged nanocomposite. So, the diffused hard segment in PUG-C vis-à-vis pure PU and PUG-P enhances the degradation kinetics to higher temperature. However, crystalline nature (grains) of amine functionalized graphene is evident in its surface morphology through SEM while cloth like morphology is clearly observed in nanocomposites indicating their amorphous behavior (Figure 4.6b). Uniform distribution of graphene sheet is also observed in PUG-C as compared to PUG-P as previously noticed through TEM bright field image.

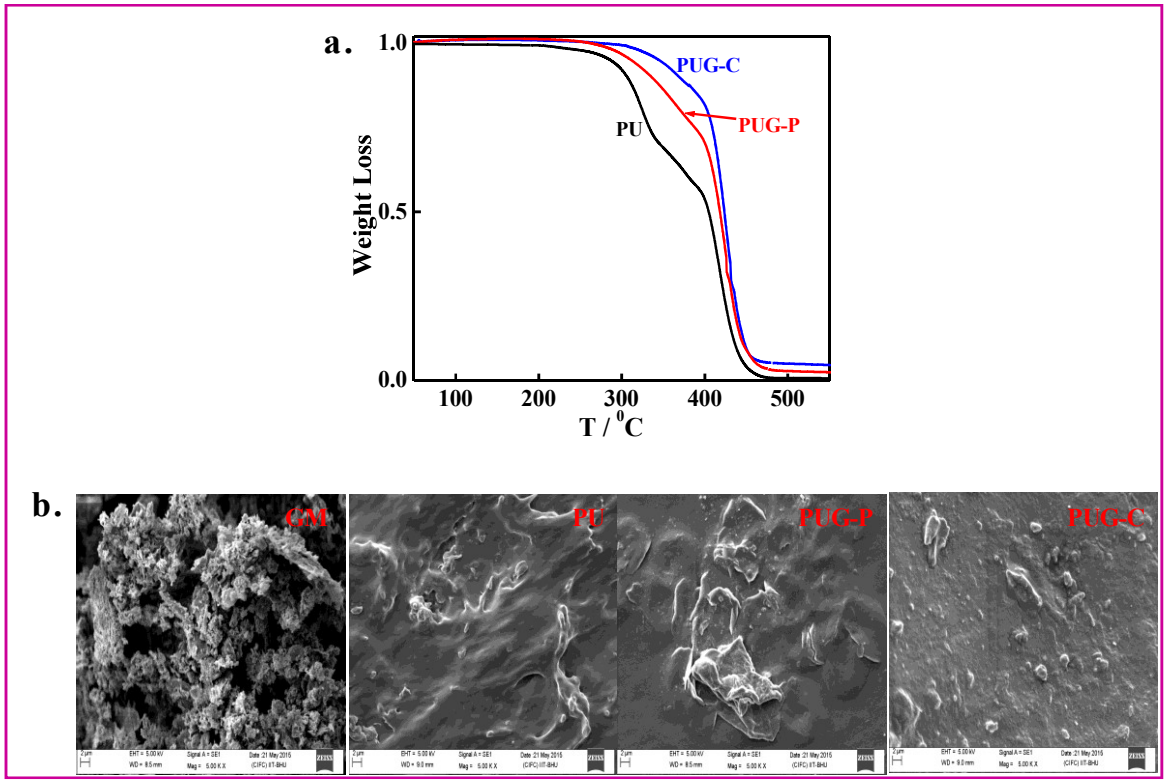

Figure 4.6: (a) TGA curve of the pure polymer and its nanocomposites and **(b)** SEM image of modified graphene with physically and chemically tagged nanocomposites.

4.2.4 Graphene induced toughening in polyurethane:

Mechanical strength through uniaxial stretching of polyurethane and its nanocomposites are presented in (Figure 4.7a). Nanocomposites exhibit the higher elongation at break as compared to the pure polymer and chemically tagged graphene nanocomposite show much higher elongation at break as compared to PUG-P. Toughness, as measured from the area under the stress-strain curve, increases for nanocomposites as compared to pure polymer (Figure 4.7b). Further, this enhancement in toughness is more pronounced in chemically tagged nanocomposites as compared to the physically mixed nanocomposites. Easy orientation of the modified graphene sheets towards the applied force is facilitated in case of chemically tagged nanocomposite where graphene sheets are the part of polymer chain and this reorganization of graphene consume the energy and thereby suppressed the crack propagation process, the key factor for the enhancement of toughness in PUG-C. On the other hand, physically mixed graphene also reorganize itself a bit due to frictional force leading to considerable increase in toughness in PUG-P [Patel et al. (2015); Mishra et al. (2014)]. Initial slope of the stress-strain curves of nanocomposites reduces significantly as compared to pure PU leading to lowering of Young's modulus of nanocomposite. The higher modulus of PU is explained from its greater crystallinity where organized hard segments act as reinforcing agent (Figure 4.7c). This is worth mentioning that crystallinity in hard segmented zone considerably reduces in PUG-C (as observed through DSC and XRD measurements) which make this system softer (low modulus) and greater amorphous content enhances its elongation at break to higher extent.

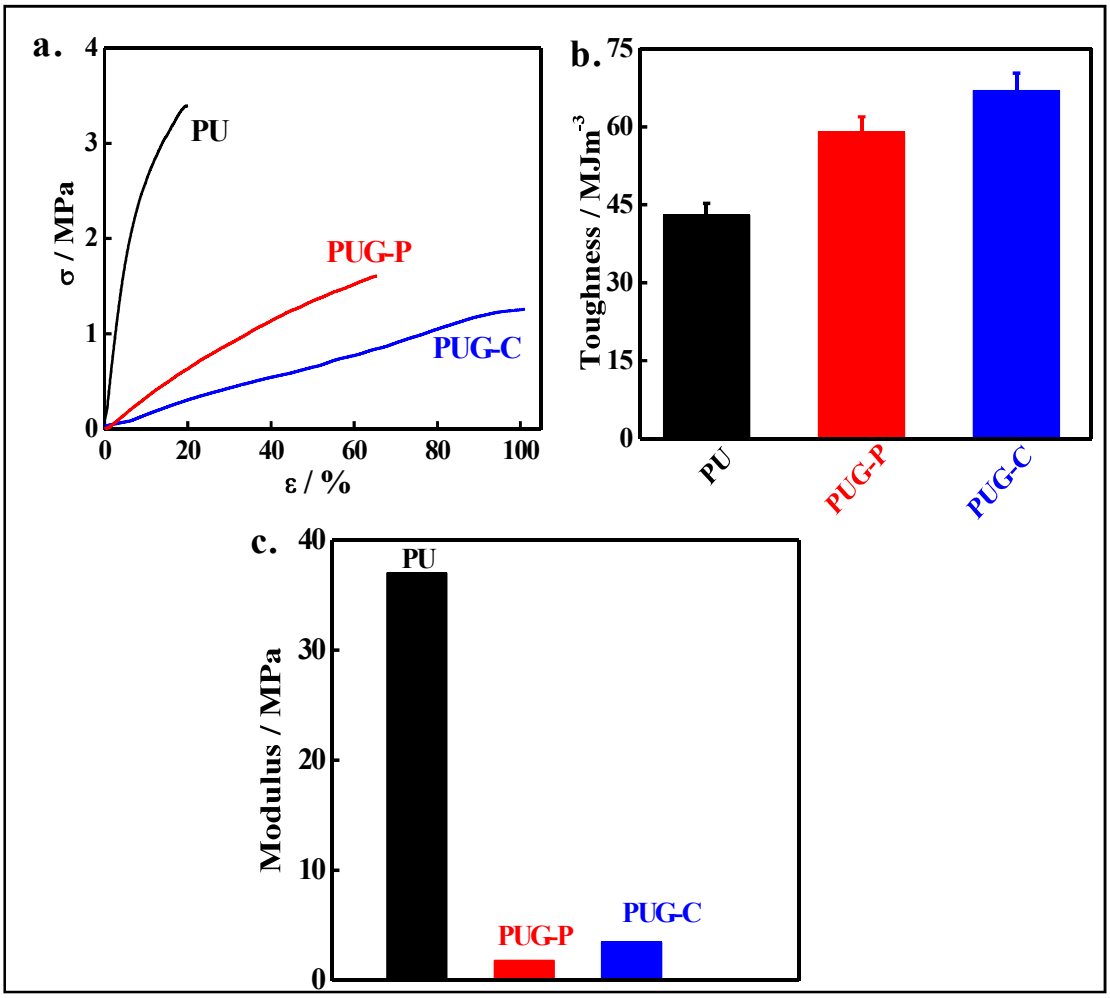

Figure 4.7: Mechanical behavior of the polymer and its nanocomposites. **(a)** Stress-stain curve of the polymer and its nanocomposites. **(b)** Toughness of the pure polymer and its indicated nanocomposites and **(c)** Modulus of pure polyurethane and its nanocomposites in bar diagram.

4.2.5 Graphene induced self-assembly in polyurethane:

Aliphatic polyurethane is known for its molecular aggregation through the hydrogen bonded interactions between the hard segments of neighboring molecules. Pure PU exhibits X-ray diffraction peak at ~6.3° corresponding to the d-spacing of 1.42 nm indicating the interplanar distance formed by the molecular sheet (Figure 4.8a) [Mishra et al. (2010)]. The peak position remains same in physically mixed graphene

nanocomposites while considerable shift in peak position occurs for chemically tagged nanocomposte towards higher angle (lower d-spacing; 1.2 nm) suggesting closer association of molecular sheet in presence of graphene. Further, humps in the small angle neutron scattering (SANS) patterns are observed at q ~ 0.4 nm^{-1} corresponding to the characteristic length, Λ_c ($=2\pi/q_m$) of 15.7, 13.5 and 13.4 nm for pure PU, PUG-P and PUG-C, respectively (Figure 4.8b). This is worth mentioning that couple of molecular sheets assembled together to form greater aggregation and the distance between those two adjacent layers is of the order of ten nanometers. Further, decreasing characteristic length for nanocomposite as compared to pure PU is explained from the fact that assembly takes with minimum number of polymer chains in presence of graphene sheet in nanocomposite while larger number of polymer chains are required to form the aggregate. Hence, graphene sheet in nanocomposite help the self-assembly process. Lowering of characteristic length in presence of layered silicate is also reported in our previous works but graphene also facilitate the molecular self-assembly [Mishra et al. (2010); Patel et al. (2015); Mishra et al. (2014)]. Moreover, the correlation lengths (ξ) were calculated from the SANS patterns using the Debye-Bueche equation (1) which provide the value in the range of 0.8, 1.23 and 1.47 nm for PU, PUG-P, PUG-C, respectively.

$$I(q) = I(o) / (1+ \xi^2 q^2)^2 \qquad (1)$$

where, I(q) is the scattered intensity, I(o) is the extrapolated structure factor at zero wavevector, q is the wavevector, and ξ is the correlation length. Debye-Bueche fitting for calculation of the correlation length is given inset of (Figure 4.8b).The correlation

length is associated with the blob size and relatively higher size in nanocomposite is presumably due to the insertion of graphene sheets within the agglomerates. In comparison with other nanofiller *e.g.* layered silicates, the lower correlation length in graphene containing nanocomposite arises from the difference in interactions between the components [Mishra et al. (2014)]. The higher order self-assembly is observed through AFM topography where 212 nm inhomogeneities are clearly noticed in pure PU whose dimension reduces to 245 nm in nanocpmposite (Figure 4.8c). The greater self-assembly is evident in optical images with the dimension of 2.3, 2.9 and 3.1 μm for pure PU, PUG-P and PUG-C, respectively (Figure 4.8d). Now, it is pertinent to understand the gradual increase of assembly size from 1.4 nm → 15 nm → 212 nm →2.3 μm observed through XRD, SANS, AFM and POM measurements where one order increase of assembly size is noticed in every step. This is to mention that extensive hydrogen bonding help the self assembly to form bigger agglomerates discernable in optical microscopy starting from nanometer dimension of molecular sheet step by step. However, macroscopic dimension of self-assembly in graphene nanocomposite is bit larger in size as compared to pure PU even though the initial assembly size is less in nanocomposites. Hence, graphene sheets influence the aggregation of polyurethane layer-by-layer self-assembly and alter the biological activity of polyurethanes.

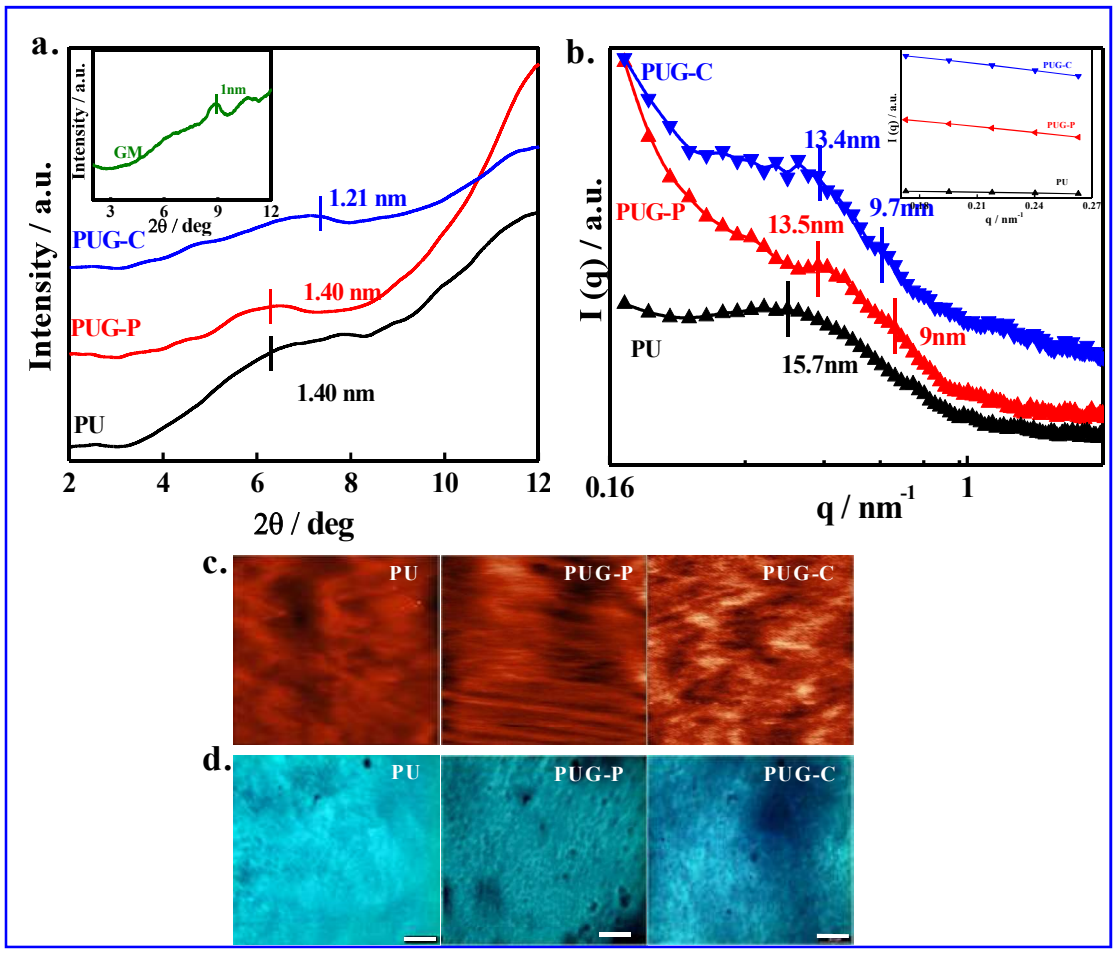

Figure 4.8: (a) XRD pattern of pure PU and its indicated nanocomposites (inset XRD pattern of amine modified graphene). **(b)** Small- angle neutron scattering patterns of the pure PU and its nanocomposites (inset Debye-Bueche fitting for calculation of the correlation length (ξ). **(c)** AFM image of the polymer and its nanocomposites (1μm × 1μm) and **(d)** Optical image of the pure PU and its indicated nanocomposites. (Scale bar 20 μm)

4.2.6 Enzymatic degradation:

Enzymatic degradation of pure PU and its nanocomposites using *lipase* from *Pseudomonas cepacia* has been presented in (Figure 4.9). Weight loss is considered to be a measure of biodegradation. Pure polyurethane shows considerable higher rate of biodegradation as compared to nanocomposites or in other words, the biodegradation rate is significantly suppressed in nanocomposite. Further, the rate of biodegradation is slowed down in chemically tagged graphene nanocomposite as compared to physical mixture of graphene in nanocomposite. It is well known that amorphous zone is prone to hydrolysis by the enzyme and higher crystallinity of nanocomposite in the soft segment zone make them less prone to biodegradation. Though the crystallinity of hard segment decrease in nanocomposite while the proximity of graphene sheet adjacent to the urethane linkage restrict somehow the hydrolysis rate leading to lower rate of biodegradation. Since lipase is hydrolytic in nature it usually attack the more sensitive amorphous zone of polymer for the biodegradation [Mishra et al. (2014)]. However, lower rate of biodegradation for nanocomposite is partly responsible for slower drug release against faster drug release in pure PU, being facilitated through higher rate of biodegradation where diffusion of drug occurs easily. Other nanofillers including layered silicates also show sluggish biodegradation rate as compared to pure polymer but the extent of slower biodegradation is more in case of graphene based nanocomoosites. Moreover, uniformly dispersed graphene in chemically tagged nanocomposite exhibits more sluggish behavior vis-à-vis PUG-P.

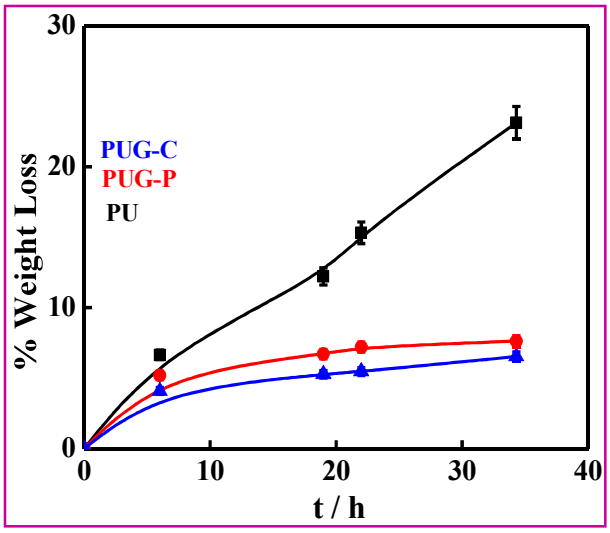

Figure 4.9: Enzymatic degradation of the pure polymer and its indicated nanocomposites through lipase (*Pseudomonas cepacia*)

4.2.7 Sustained drug delivery:

In vitro drug release in phosphate buffer solution (pH~7.4) at 37 ºC has been studied using dexamethasone drug embedded in pure PU and its nanocomposites. The concentration of the released drug from the polymer and its nanocomposites were measured through the UV-visible absorption studies [Schierholz et al. (1997); Depan et al. (2009)]. Standard curve was drawn after taking absorbance using 242 nm in concentration range of 5-100 µg/ml and concentration of release drug was measured through UV-visible absorbance. Standard curve of drug is given in (Figure 4.10).

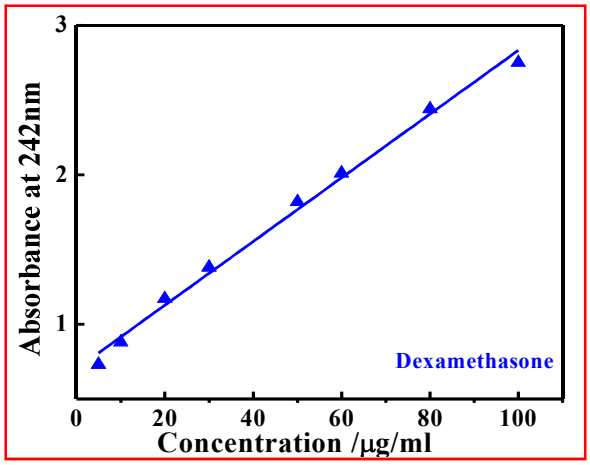

Figure 4.10: Standard curve of Dexamethasone standard stock solution (1mg/ml) drawn after taking absorbance using UV-visible spectrometer at 242 nm in the concentration range of 5-100 µg/ml.

The cumulative percentage release of dexamethasone drug as a function of time is presented in (Figure 4.11a). Around 15% burst released, arise from the surface adhered drug, is noticed in pure PU which reduces to 10% in nanocomposites. Interestingly, overall drug release kinetics has been sustained in nanocomposites as compared to pure PU and chemically tagged graphene nanocomposite exhibits significant sustained release. There are various steps to determine drug release from polymer matrix i) penetration of the liquid into the matrix, ii) dissolution of drug and, iii) diffusion of drug from the matrix and any of these steps may be the rate determining step for the overall release kinetics [Singh et al. (2011)]. To understand the mechanism, the release kinetics of dexamethasone are best fitted with Korsmeyer-Peppas model (r^2~0.998) leading to exponent '*n*' values of 0.54, 0.70 and 0.72 for pure polymer, PUG-P and PUG-C, respectively, indicating non-Fickian ($n \geq 0.45$) behavior of drug release (Figure 4.11b). Sustained release of loaded drug in nanocomposites is due to diffusion out of drug through a tortuous path in presence of two dimensional graphene sheets dispersed in polymer matrix. Further, the greater self-assembly in nanocomposites

hinders the release kinetics causing sustained release. Moreover, homogeneous dispersion of graphene sheets helps sustained release of drug in PUG-C vis-à-vis PUG-P where agglomeration of graphene reduces the tortuous path. A schematic representation of drug release is shown in (Figure 4.11c) indicating the tortuous path in two different nanocomposites which cause differential release rate. However, chemically tagged nanocomposites exhibits higher exponent value as compared to pure polymer and PUG-P indicating slow release due to the presence of two dimensional graphene sheets. This is to mention that release kinetics have been fitted with other models but Korsmeyer-Peppas model is found to be the best fitted one as reveled from its highest r^2 value (Table 4.1). The rate of biodegradation may also affect the release kinetics and needs to look upon.

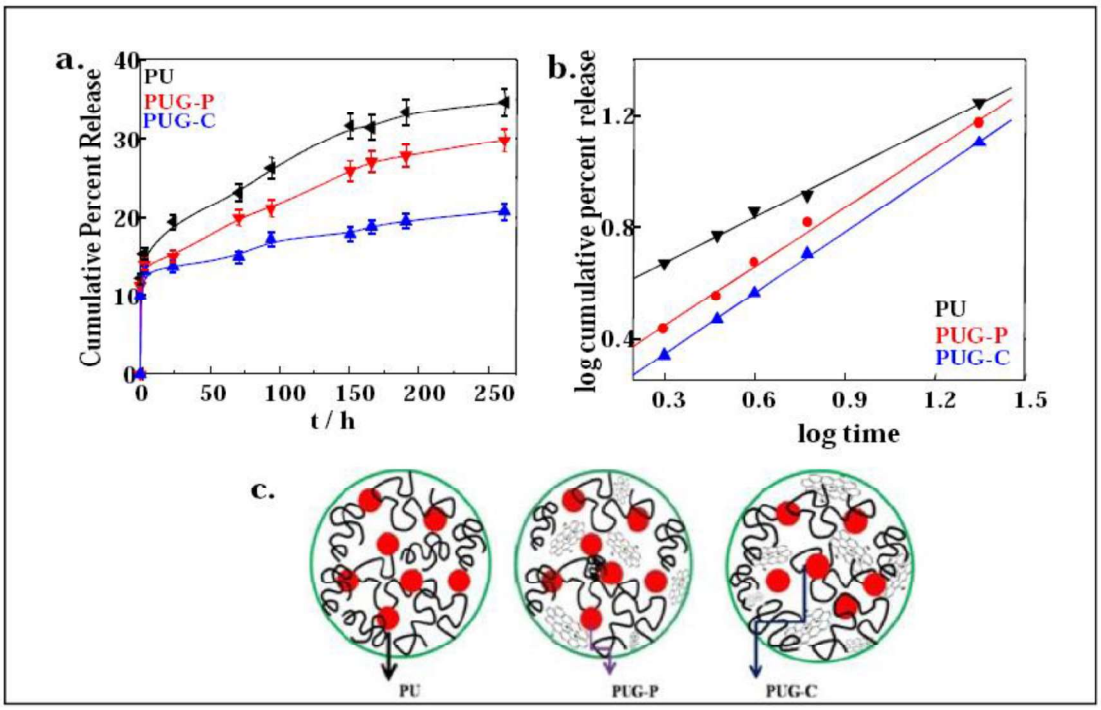

Figure 4.11: (a) Sustained drug release profile of indicated PU and its nanocomposites. **(b)** Korsemeyer- Peppas model for mechanism of drug release in PU and its indicated nanocomposites and **(c)** Schematic model of drug release kinetics. The black line represents the polymer chains whereas plates indicate the graphene sheets. Arrow shows the probable path for drug diffusion.

Sample	Zero Order		First Order		Higuchi		Korsmeyer-Peppas	
	k	r^2	*k*	r^2	*k*	r^2	n	r^2
PU	0.61 0.03	0.995	0.003 0.00013	0.991	3.95 0.11	0.993	0.54 0.01	0.998
PUG-P	0.57 0.04	0.992	0.0033 0.00012	0.990	3.72 0.06	0.994	0.70 0.03	0.996
PUG-C	0.50 0.02	0.990	0.0024 0.0001	0.994	3.2 0.07	0.991	0.72 0.01	0.999

Table 4.1: Table for release rate constant (*k*), correlation coefficient (r^2) and diffusion release exponent (*n*) obtained using different mathematical models for drug loaded PU and its indicated nanocomposites.

4.2.8 Cell viability:

Being able to release the biological molecules in a controlled way, it is necessary to study the biocompatibility of these nanocomposites using cell line. Cell viability of the HeLa cells on the surface of pure PU and its nanocomposites has been studied through MTT assay. Cells cultured without polymeric material was taken as control. Cell viability on pure PU is higher than its nanocomposites after 1 day of culture while cell viability increases rapidly with time (Figure 4.12a). Cell viability of nanocomposites almost equals to that of pure PU after 5 days of culture. Interestingly, chemically tagged nanocomposites exhibit higher cell viability as compared to physically mixed graphene nanocomposites. Polyurethanes are known for their biocompatibility and are being used for many different applications but graphene is not so biocompatible [Yang et al. (2013)]. In contrast, nanocomposites are found to be biocompatible after wrapping up of the graphene sheets with compatible polymer. Further, PUG-C shows better cell viability as compared to PUG-P as the graphene sheet are better enfold, being the part of polymer chain. This result indicates that nanocomposites having chemically tagged graphene as filler material exhibits better cell growth as compared to the nanocomposites of physically mixed graphene. Oxidized graphene nanoribbons formed through the longitudinal unzipping of CNTs in PEG-DSPE (1,2-distearoyl-sn-glycero-3-phosphoethanolamine-N-[amino(polyethylene glycol)]) matrix exhibit decrease in cell viability of HeLa cells after 24 and 48h while amine functionalized graphene nanocomposites of polyurethane show much better biocompatibility [Chowdhury et al. (2013)]. Biocompatibility of the amine modified graphene oxide in

terms of thrombotoxicity was evaluated by Singh et al. using the blood platelets [Singh et al. (2012)]. Combining our previous studies and some literature reported information it appears that amine functionalized graphene help improving the biocompatibility of the nanocomposites towards HeLa cell. This observation is further supported through the fluorescence image of the cells using acridine orange and ethydine bromide dye (Figure 4.12b). Cells are healthier on chemically tagged nanocomposites as compared to pure PU and physically mixed graphene nanocomposites. It was also reported that differentiation of the cells were occurred in surface of graphene oxide [Ku et al. (2013)].

4.2.9 Cell adhesion:

Carbon materials are frequently used as implant material and in tissue engineering field due to their inherent biocompatible nature [Harrison et al. (2007); Duarte et al. (2004)]. Cells need to be adhered on top of implant materials for better growth. Cell adhesion of HeLa cell on pure PU and its nanocomposites are presented in (Figure 4.12c). It is clearly observed that chemically tagged graphene nanocomposite exhibit better cell adhesion behavior as compared to pure PU and physically mixed graphene nanocomposite. Since, biocompatible polyurethane is frequently used as an implant material as well as in biomedical device, chemically tagged nanocomposites is a better choice with its improved physical properties along with the greater biological activities in terms of cell viability and cell adhesion [Hung et al. (2009); Rinaldo et al. (2007)]. Further, cell adhesion in PUG-C is found to be much greater than that of PUG-P indicating chemical tagging is better approach for nanocomposite preparation.

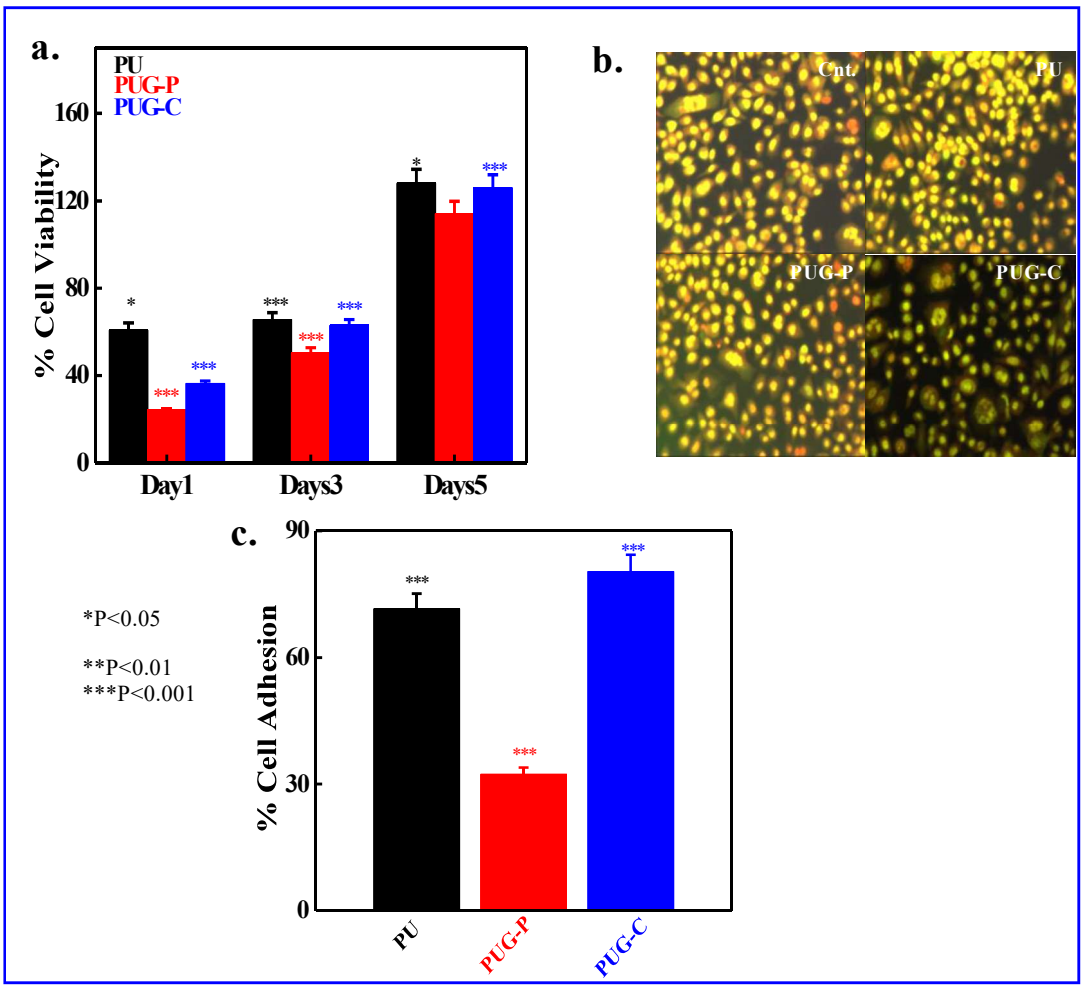

Figure 4.12: Biological studies on pure PU and its indicated nanocomposites. **(a)** HeLa cell viability of pure PU and its nanocomposites with time interval of 1, 3 and 5 days; **(b)**Fluorescence microscopic image of cell cultured on PU and its indicated nanocomposites after 1 day of cell proliferation and **(c)** HeLa cell adhesion on PU and its indicated nanocomposites.

4.3 Conclusions:

Graphene nanocomposites with polyurethane have been synthesized using functionalized graphene as chain extender. The chemical tagging of graphene within the polyurethane chain is confirmed through NMR studies. The superior properties of chemically tagged nanocomposites have been compared with physically dispersed functionalized graphene nanocomomposite. Dispersion of graphene platelets is homogeneous and uniform in chemically tagged nanocomposite as opposed to the agglomerated nanostructure noticed in physically mixed graphene nanocomposite observed through bright field TEM images. Greater interaction in chemically tagged nanocomposite has been revealed through FTIR, UV-visible and PL spectroscopic techniques and the result are compared with physically tagged nanocomposite. Graphene as a part of polymer chain in nanocomposite makes this difference of dispersion and interaction which in turn enhances the thermal stability and toughening behavior of nanocomposite as compared to pure polyurethane and physically tagged nanocomposite. Graphene platelets induce self-assembly in polyurethane through close association with the polymer chain and greater interactions as observed through step by step self-assembly starting from nanometer to micron size cluster as observed through XRD, SANS, AFM and optical microscope. The effect of self-assembly has been reflected in drug delivery causing sustained release in chemically tagged nanocomposite vis-à-vis pure polyurethane due to tortuous path in presence of self-assembled inhomogeneities and two-dimensional graphene platelets. Biocompatibility of this nanocomposite has been explored through cell viability, cell adhesion and

fluorescence image indicating better biocompatible material in comparison to physically graphene tagged nanocompoosites. However, control releases of cancerous drug as well as the biocompatible nature of chemically tagged nanocomposites with its superior thermal and mechanical properties make it an attractive biomaterial for drug delivery and tissue engineering applications.